Nicotinic Acetylcholine Receptor Induces Lateral Segregation of Phosphatidic Acid and Phosphatidylcholine in Reconstituted Membranes†

Jorge J. Wenz and Francisco J. Barrantes*

UNESCO Chair of Biophysics and Molecular Neurobiology and Instituto de Investigaciones Bioquímicas de Bahía Blanca, B8000FWB Bahía Blanca, Argentina

Received September 13, 2004; Revised Manuscript Received October 20, 2004

ABSTRACT: Purified nicotinic acetylcholine receptor (AChR) protein was reconstituted into synthetic lipid membranes having known effects on receptor function in the presence and absence of cholesterol (Chol). The phase behavior of a lipid system (DPPC/DOPC) possessing a known lipid phase profile and favoring nonfunctional, desensitized AChR was compared with that of a lipid system (POPA/POPC) containing the anionic phospholipid phosphatidic acid (PA), which stabilizes the functional resting form of the AChR. Fluorescence quenching of diphenylhexatriene (DPH) extrinsic fluorescence and AChR intrinsic fluorescence by a nitroxide spin-labeled phospholipid showed that the AChR diminishes the degree of DPH quenching and promotes DPPC lateral segregation into an ordered lipid domain, an effect that was potentiated by Chol. Fluorescence anisotropy of the probe DPH increased in the presence of AChR or Chol and also made apparent shifts to higher values in the transition temperature of the lipid system in the presence of Chol and/or AChR. The values were highest when both Chol and AChR were present, further reinforcing the view that their effect on lipid segregation is additive. These results can be accounted for by the increase in the size of quencher-free, ordered lipid domains induced by AChR and/or Chol. Pyrene phosphatidylcholine (PyPC) excimer (E) formation was strongly reduced owing to the restricted diffusion of the probe induced by the AChR protein. The analysis of Förster energy transfer (FRET) from the protein to DPH further indicates that AChR partitions preferentially into these ordered lipid microdomains, enriched in saturated lipid (DPPC or POPA), which segregate from liquid phase-enriched DOPC or POPC domains. Taken together, the results suggest that the AChR organizes its immediate microenvironment in the form of microdomains with higher lateral packing density and rigidity. The relative size of such microdomains depends not only on the phospholipid polar headgroup and fatty acyl chain saturation but also on AChR protein−lipid interactions. Additional evidence suggests a possible competition between Chol and POPA for the same binding sites on the AChR protein.

The diversity of lipids in biological membranes, with differences in hydrocarbon chain, polar headgroups, and backbone structure, and the accurate regulation of their content and composition by cells point to the key role of lipids in cellular physiology in general and membrane structure and function in particular. The functionality of membrane proteins, related to their conformation in the membrane, is also dependent on membrane lipid composition.

The nicotinic acetylcholine receptor (AChR),[1] the archetype molecule in the superfamily of ligand-gated ion channels, is an oligomeric multispanning transmembrane protein. Despite the extensive information gained on the functional and to some extent structural dependence of the AChR on its surrounding lipids (see reviews in refs *1* and *2*), several aspects of the modulation exerted by different lipid classes on the AChR still remain unclear. Various mechanisms have been implicated in the modulation of AChR function by lipids: (i) direct effects, exerted through binding to specific sites on transmembrane portions of the protein (*3*−*6*), in some cases entailing allosteric modulation of such sites; (ii) modification of bilayer physical properties, such as fluidity, membrane curvature, and/or lateral pressure (*5*, *7*−*9*); and (iii) promotion of lateral segregation of specific lipids and formation of lipid domains having optimal packing density (*10*, *11*).

In recent years, the "raft" hypothesis has proposed that Chol and (glyco)sphingolipid-enriched microdomains act as platforms for the sorting of membrane components such as glycosylphosphatidylinositol-anchored proteins (GPI-APs), which appear to partition preferentially into ordered lipid domains (*12*−*14*). The aggregation and cluster size of a GPI-AP have been reported to be affected by lipid domains and Chol levels (*15*). In the particular case of the AChR, early work suggested that in rat myotubes the AChR occurred in

† This work was supported in part by grants from the Universidad Nacional del Sur and FONCYT, Argentina.

* To whom correspondence should be addressed. Phone: (++54) 291 486-1201. Fax: (++54) 291 486-1200. E-mail: rtfjb1@criba.edu.ar.

[1] Abbreviations: AChR, acetylcholine receptor; Chol, cholesterol; DPH, diphenylhexatriene; DOPC, dioleoylphosphatidylcholine; DPPC, dipalmitoylphosphatidylcholine; POPC, 1-palmitoyl-2-oleoylphosphatidylcholine; POPA, 1-palmitoyl-2-oleoylphosphatidic acid; MLV, multilamellar vesicles; *r*, anisotropy; SLPC, nitroxide spin-labeled 1-palmitoyl-2-stearoyl-(doxyl)-*sn*-glycero-3-phosphocholine; PA, phosphatidic acid; DTNB, 5,5′-dithiobis(2-nitrobenzoic acid); PyPC, 1-hexadecanoyl-2-(1-pyrenedecanoyl)-*sn*-glycero-3-phosphocholine; T_m, transition temperature; *F*, fluorescence intensity; FRET, Förster energy transfer.

10.1021/bi048026g CCC: $30.25
Published on Web 12/08/2004

lipid domains having a composition distinct from the rest of the muscle membrane (*16*). The AChR protein is surrounded by boundary ("annular", "shell") lipid (*17*, *18*) that is immobilized relative to the bulk bilayer lipid in native membranes derived from the *Torpedo* postsynapse. This lipid microenvironment has a lesser degree of water penetration than the bulk lipid bilayer and has the characteristics of the liquid-order (l_o) lipid state (*19*), similar to those purported to occur in raft lipid domains. Poveda and co-workers (*11*) recently reported that the AChR affects phospholipid organization in reconstituted Chol-containing liposomes by directing lateral phase separation of certain phospholipids such as phosphatidic acid (PA), but not of others (PG, PC, PE), causing the formation of lipid domains segregated from the bulk lipid matrix. Incorporation of AChR into pure phosphatidylcholine (PC) liposomes stabilizes the AChR in a nonresponsive, desensitized state, whereas reconstitution into PA- or Chol-containing liposomes favors a functional, resting state of the AChR (*10*). There is an increase in both the lateral packing density and phase transition temperature of reconstituted bilayers composed of POPC/DOPA or POPC/POPA but not of those composed of POPC only (*10*).

The high Chol content of native AChR-rich membranes (see review in ref *20*) and the l_o lipid phase-promoting ability of Chol further suggest that AChR functionality may be at least in part associated with the formation and/or the extent of such ordered lipid phase. That the maintenance of an ordered lipid phase in the AChR microenvironment is important for receptor function is further corroborated by the detrimental effect on AChR single-channel activity by steroids (*21*−*25*), the majority of which impair lipid domain formation and reduce the extent of the l_o phase (*26*).

In the present work we reconstituted purified AChR protein into synthetic membranes with various lipid compositions in the presence and absence of Chol. Fluorescence studies, including fluorescence quenching of DPH extrinsic fluorescence and AChR intrinsic fluorescence by a nitroxide spin-labeled phospholipid, anisotropy of the probe DPH, excimer (E) formation of a fluorescent PC (pyrene−phosphatidylcholine, PyPC), and Förster energy transfer (FRET) from the protein to either DPH or PyPC, were carried out to investigate the distribution in, and the effect of AChR protein on, the lipid organization in the reconstituted membranes. The phase behavior of a lipid system (DPPC/DOPC) possessing a known phase profile (see, e.g., review in ref *27*) and functional effects on the AChR protein (*5*) were compared with that of a lipid system (POPA/POPC) containing PA, an anionic phospholipid with the ability to modulate the functional state of the AChR by stabilizing it predominantly in a resting-like state (*3*, *5*, *10*, *28*, *29*). Our results show that incorporation of the AChR increases the proportion and rigidity of the ordered lipid phase. The relative fraction of the ordered phase is also found to depend on the polar headgroup and saturation of the fatty acid acyl chains of the host lipid in which the AChR is reconstituted.

EXPERIMENTAL PROCEDURES

Materials

Electric fish (*Torpedo californica*) were obtained from Aquatic Research Consultants (San Pedro, CA) and stored at −70 °C until further use. DPPC, DOPC, DPH, Chol, and cholic acid were purchased from Sigma Chemical Co. (St. Louis, MO). POPA, POPC, and nitroxide spin-labeled PCs (7- and 10-SLPC) were obtained from Avanti Polar Lipids (Alabaster, AL). PyPC were obtained from Molecular Probes Inc. (Eugene, OR). Midrange protein molecular weight markers were purchased from Promega (Madison, WI). All other reagents were of analytical quality. Lipid stock solutions were prepared in chloroform/methanol (2:1 v/v) at a final concentration ranging between 0.5 and 1 mg/mL and 0.01 mg/mL for DPH. All solutions were stored at −20 °C before use.

Methods

Purification of the AChR Protein. All steps were carried out at 4 °C. Crude membranes from electric tissue of *T. californica* were prepared as described previously (*30*). The receptor was purified from crude membranes by affinity chromatography using Affi-Gel 10 resin (Bio-Rad Laboratories, Hercules, CA) previously activated as described elsewhere (*31*) with slight modifications. Briefly, the affinity column was prepared by coupling cystamine to the matrix, reduction of disulfide bonds with dithiothreitol, and a final activation with bromoacetylcholine bromide. Derivatization of the gel was followed qualitatively in each step by assaying for sulfhydryl groups with DTNB. The activated gel was stored at 4 °C and used within 1 month.

Crude membranes with a protein concentration of 6−7 mg/mL were obtained from 90 g of electric tissue, made to a protein concentration of 2 mg/mL in buffer A [10 mM phosphate, 100 mM NaCl, 0.1 mM EDTA, 0.2% sodium azide (w/v), pH 7.4]. The membranes were solubilized by adding cholic acid to give a final concentration of 1% (w/v) with gentle stirring for 20 min. The detergent extract was centrifuged in a Ti 70 type rotor at 34000 rpm for 45 min. After 10 mL of the activated affinity column was washed with 4−5 volumes of water followed by 2 volumes of buffer A with 1% cholate, the supernatant was applied to the column. To exchange native lipids with the desired exogenous lipids (reconstitution), the column was preequilibrated with the following sequence of DPPC or POPA/POPC (1:3 mol/mol) solutions in buffer A containing 1% cholate: 4 volumes of 0.1 mg/mL, 2.5 volumes of 2 mg/mL, and 3 volumes of 0.1 mg/mL. The AChR was eluted by applying 3 volumes of buffer A containing 1% cholate, 10 mM carbamoylcholine, and 0.1 mg/mL DPPC or POPA/POPC (1:3 mol/mol). The protein concentration was monitored by A_{280}, and fractions with values higher than 0.1 were pooled. To eliminate cholate and carbamoylcholine and in order to form vesicles, the mixture was dialyzed using M_w 12000 cutoff cellulose membranes at 4 °C against 200 volumes of buffer A, with gentle stirring for 40 h and buffer replacement every 8 h.

Characterization of Purified AChR. The protein concentration was assayed according to ref *32*. Lipids were extracted as described in ref *33* and assayed for inorganic phosphorus content (*34*). Total lipid concentration was 0.12 mg/mL (0.163 mM). To verify the purity of the AChR, SDS gel electrophoresis was performed under denaturing conditions (35) using 0.75 mm thick gels and 10% total acrylamide concentration. Electrophoresis was carried out in a Mini Protean II cell (Bio-Rad) for 3 h at 15 mA, supplied by a

Table 1: Composition and Final Lipid Concentrations in the Liposomes Used in Fluorescence Experiments[a]

		molar ratio							
		DPPC/DOPC				POPA/POPC			
		F_0	F	F_0	F	F_0	F	F_0	F
without AChR	DPH	1	1	1	1	1	1	1	1
	DPPC	41	41	41	41				
	POPA					73	73	73	73
	DOPC	59		59					
	POPC					27		27	
	7-SLPC		59		59		27		27
	Chol			20	20			27	27
	final lipid concn (μM)	27	27	35	35	29	29	37	37
with AChR	DPH	1	1	1	1	1	1	1	1
	DPPC	60	60	60	60				
	POPA					60	60	60	60
	DOPC	40		40					
	POPC					40	20	40	20
	7-SLPC		40		40		20		20
	Chol			20	20			20	20
	final lipid concn (μM)	40	40	48	48	40	40	48	48

[a] F_0 and F correspond to the fluorescence intensity in the absence and presence of nitroxide spin-labeled quencher, 7-SLPC, respectively. Quenching was accomplished by replacing all or one-half of the phospholipid with the lowest T_m (DOPC or POPC) by an equal amount of 7-SLPC. Background fluorescence was measured in liposome samples (DPPC/DOPC or POPA/POPC at 50:50 molar ratio) with a final lipid concentration of 40 μM. Compositions shown in the lower panel were achieved by incorporation of AChR into the liposomes listed in the upper panel, resulting in a final lipid to protein molar ratio of 500:1. Similar compositions and final lipid concentrations (but lacking quencher) were used in the sets of experiments with PyPC as fluorescence lipid (see figure legends for detailed composition of liposomes).

Power Pack 3000 (Bio-Rad). AChR subunits were visualized using a silver staining kit (Amersham, Uppsala, Sweden) and were identified by comparison with midrange protein molecular weight markers.

Liposome Preparation and Rereconstitution of Purified AChR. Multilamellar vesicles (MLV) were prepared by mixing the appropriate amount of stock solution of each component to obtain the desired composition in each lipid system (DPPC/DOPC or POPA/POPC) (Table 1). Lipid:protein ratios were calculated and adjusted in order to achieve the desired lipid and protein concentrations upon incorporation of AChR into the liposomes. The mixtures were dried under nitrogen at room temperature while rotating the round-bottomed tubes to form the lipid film. Samples were then dehydrated under nitrogen for 1 h to eliminate the remaining solvent. Buffer A was added to the thin lipid film and heated to 48−50 °C (i.e., at a temperature higher than the highest T_m of the constitutive lipids). At this stage, the total lipid concentration of the suspension was 0.5 mg/mL. The samples were then vigorously vortexed in two steps of 1 min each, also at 48−50 °C, and incubated for 30 min in a low-power bath sonicator in order to obtain a more uniform size distribution of the resulting MLVs. Before fluorescence measurements, samples were diluted with buffer A to the desired final lipid concentration (Table 1).

The purification procedure yielded membranes with a lipid to protein ratio of 160:1 (mol/mol). Purified AChR protein (0.25 mg/mL) was added to aliquots of liposomes, giving rereconstituted membranes with a lipid to protein ratio of 500:1 (mol/mol) and with the composition given in Table 1. Detergent solubilization was carried out at 4 °C by addition of cholic acid (25% w/v) to obtain a final detergent concentration of 1% (w/v) followed by two vortexing steps of 1 min each. The preparation of AChR-containing vesicles was accomplished by dialysis at 4 °C, as described above. Liposomes otherwise identical to the AChR-containing ones (lower panel in Table 1), but lacking the protein, and other pure lipid liposomes composed only of 40 μM DPPC, DOPC, POPA, or POPC were prepared using the same procedure. When assayed by [^{125}I]-α-bungarotoxin binding the specific activity of the reconstituted membranes fell within the expected values (see, e.g., refs *5* and *11*).

Fluorescence Measurements. Fluorescence emission spectra and fluorescence anisotropy measurements were recorded with an SLM 4800 ISC spectrofluorometer (SLM Instruments, Urbana, IL) using a vertically polarized light beam from a Hannovia 200 W mercury/xenon arc fitted with a Glan-Thompson polarizer (4 nm excitation and emission slits). Optimal excitation/emission wavelengths for DPH, PyPC, and AChR were 358/424, 340/374−474, and 290/330 nm, respectively. Measurements were carried out in 5 × 5 mm quartz cuvettes at increasing temperatures (0−58 °C). A 418 nm cutoff filter (KV418; Schott, Mainz, Germany) was used for the measurement of DPH anisotropy. Fluorescence data were obtained from duplicate or triplicate independent experiments 10−15 min after the desired working temperature was reached. The heating rate was 0.5°/min; temperature was regulated by a thermostated circulating water/methanol bath (Haake, Darmstadt, Germany) and monitored inside the cuvette with a thermocouple. Background fluorescence was measured from samples containing liposomes of each lipid system (DPPC/DOPC or POPA/POPC, 50:50 mol/mol, 40 μM) without quencher, fluorescence probe, or AChR. The fluorescence intensity of these background samples amounted to less than 5−10% of that of the fluorophore-containing counterpart for the protein and the two fluorophores (DPH and PyPC), respectively. In FRET experiments samples were excited at 290 nm, and fluorescence of AChR (F_{330nm}), DPH (F_{424nm}), or PyPC (F_{373nm} and F_{474nm}) was recorded from the emission spectra. The fluorescence intensity of DPH excited at the excitation wavelength of the AChR protein (290 nm) amounted to less than 3.5% of the fluorescence emission at 358 nm. In all cases, background fluorescence was subtracted from each corresponding counterpart before quenching values, FRET, or fluorescence ratios were calculated.

RESULTS

Bilayer Organization in a DPPC/DOPC/AChR System

Quenching of DPH. In a previous work (*26*) we modified and extended the procedure of London and co-workers (*36*, *37*) to investigate the effect of steroids on lipid domain formation or disruption in model membranes. This method is based on the comparison between the degree of quenching induced by a nitroxide spin-labeled phospholipid (SLPC) on the fluorescence of the extrinsic probe DPH reconstituted into membranes composed of phospholipids with different T_m (e.g., DPPC/DOPC or POPA/POPC). When membranes are made up of an unsaturated lipid (e.g., DOPC or POPC)

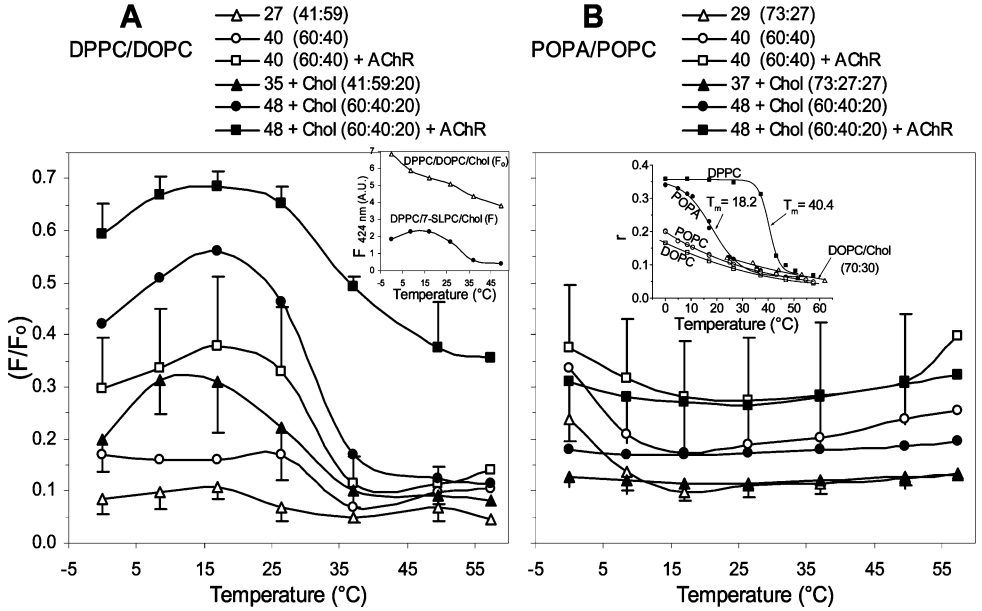

FIGURE 1: Quenching of DPH (F/F_0) by 7-SLPC, expressed as the ratio between fluorescence intensity in quencher-containing samples (F) and those devoid of quencher (F_0), having the corresponding unsaturated lipid (DOPC or POPC) instead. (A) DPPC/DOPC and (B) POPA/POPC liposomes. The final lipid concentration (μM) and the molar ratio between the two constitutive lipids (in parentheses) are given to the right of the symbols. The molar ratio of Chol in the Chol-containing liposomes is represented by the third figure in parentheses. The lipid to protein molar ratio of AChR-containing liposomes was 500:1. Error bars represent the SD of three independent experiments. Inset A: Fluorescence intensity of DPH (F_{424nm}) as a function of temperature of two selected liposomes: F sample (DPPC/DOPC/Chol, 41:59:20 mol/mol/mol, 35 μM) and F_0 sample (DPPC/7-SLPC/Chol, 41:59:20 mol/mol/mol, 35 μM). Inset B: DPH fluorescence anisotropy in liposomes of the indicated composition (final lipid concentration, 40 μM). Data sets were collected from two independent experiments at different temperatures (x-values), except for the DOPC and DOPC/Chol liposomes ($n = 1$).

and a fluorescent quencher phospholipid (e.g., 7-SLPC) having a phase behavior similar to that of an unsaturated lipid (the T_m of both lipids is below 0 °C), all components mix and distribute randomly in the bilayer at temperatures above their T_m. Since no segregation occurs between the two lipids, the majority of the fluorophore molecules are expected to have a quencher molecule in their vicinity, and the fluorescence of the system as a whole is highly quenched. When the unsaturated lipid is replaced by a saturated lipid (e.g., DPPC or POPA) and all other components remain the same, the DPPC (or POPA) molecules can eventually segregate from the quencher molecules at temperatures below their T_m. It is important to point out that DPH displays no preference for either phase (*38*) and hence distributes equally between the two. The fraction of DPH remaining in the DPPC-enriched domain exhibits a lower probability of interaction with quencher molecules, and as a result, the degree of quenching is low. As the temperature increases, the segregated lipid domain melts and mixes with the quencher, which interacts and quenches those DPH molecules that were sheltered in the DPPC domain at lower temperatures. A necessary requisite for DPH to operate as a faithful probe in this system is that its quantum yield does not depend on the phase transition of the saturated lipids. We experimentally determined that the fluorescence intensity of DPH in neat DPPC or POPA liposomes did not significantly change in the 0−58 °C temperature range, indicating that phase transition of the saturated lipid does not affect the quantum yield of DPH (data not shown), in agreement with the data of Lentz's group (*38*) on DPPC/DMPC liposomes.

Figure 1 shows the temperature dependence of DPH quenching in DPPC/DOPC (A) and POPA/POPC (B) liposomes with different lipid compositions and concentrations (Table 1) in the presence or absence of the AChR and Chol. Quenching is expressed as the ratio between fluorescence intensity in quencher-containing samples (F) and those devoid of quencher (F_0), having the corresponding unsaturated lipid (DOPC or POPC) instead. To illustrate the evolution of fluorescence intensity of DPH as a function of temperature in F and F_0 liposomes, two selected samples are shown in inset A (Figure 1). Fluorescence intensity in quencher-free samples decreased smoothly as temperature increased. On the contrary, a remarkable drop was observed in quencher-containing samples, due to the enhanced probability of contact between 7-SLPC and DPH during melting and reorganization of lipids. In quencher-free samples a similar reorganization of lipid occurred, but DOPC was not able to quench DPH. Thus, we interpret the smooth decrease in fluorescence intensity as due to the single effect of temperature on the quantum yield of DPH. The lower curve in Figure 1A corresponds to the quenching of liposomes composed of DPPC/DOPC at a 41:59 molar ratio with an overall lipid concentration of 27 μM. Addition of purified AChR to this mixture caused a decrease in fluorescence quenching (higher F/F_0 values), indicating that the AChR protein promotes the formation and/or increases the size of the DPPC domains in which DPH is sheltered from the quencher. Incorporation of the receptor (and presumably its boundary lipids) to control liposomes yields membranes with an increased overall lipid concentration (i.e., from 27 to 40 μM) and a change in the DPPC/DOPC (or 7-SLPC) molar ratio (i.e., from 41:59 to 60:40), caused by the endogenous lipid content (average 0.12 mg/mL or 0.163 mM) of the purified receptor membranes. To determine whether the reduced quenching observed after AChR incorporation was due to this enhanced lipid to quencher molar ratio or to the

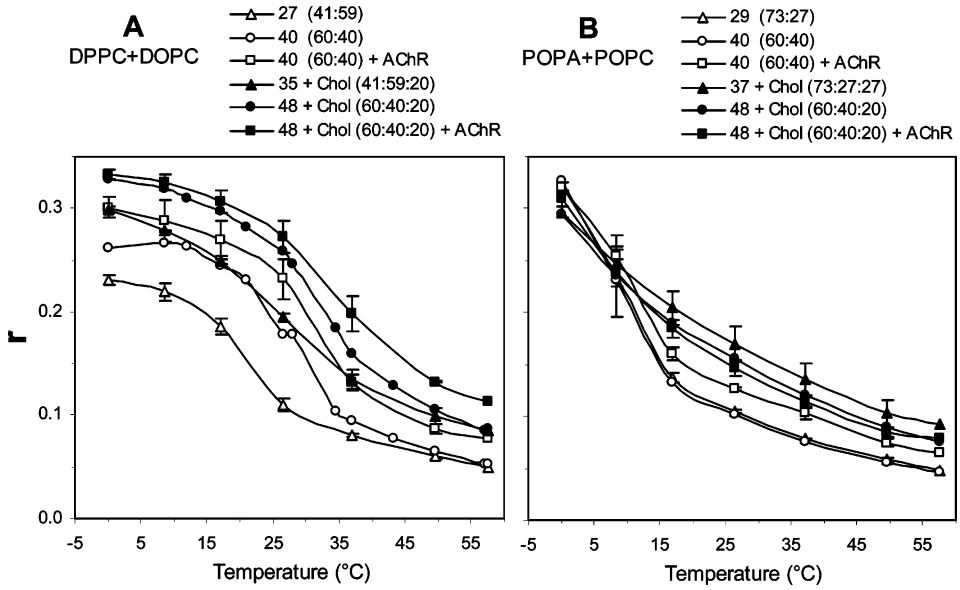

FIGURE 2: Temperature dependence of DPH fluorescence anisotropy in DPPC/DOPC (A) and POPA/POPC (B) liposomes, respectively. Error bars represent the SD of three independent experiments.

increased lipid concentration, similar liposomes having the same overall lipid concentration (40 μM) and lipid to quencher molar ratio (60:40), but lacking the AChR, were assayed next. As expected, the corresponding quenching curve was intermediate between that of the sample with lower lipid concentration and higher lipid to quencher ratio but lacking receptor and that of the same lipid composition and concentration but with AChR (Figure 1A). Taken together, these findings indicate that the AChR itself causes a reduction in quenching and that this effect is not due to a mere "dilution" of the quencher with the saturated lipid (DPPC) during the reconstitution procedure or to the increased phospholipid concentration.

Upon addition of Chol (a known lipid domain promoter) to the system, the degree of quenching was lower at any phospholipid concentration, regardless of the presence or absence of the AChR protein (Figure 1A). Again, to determine whether the effect was mediated by the receptor protein or by the increased phospholipid concentration and/or higher phospholipid/quencher molar ratio as a result of AChR protein incorporation, a sample with the same lipid/quencher molar ratio (60:40) and final lipid concentration (48 μM) as that of the AChR-containing liposomes was also assayed. As in the Chol-free samples described above, these samples displayed a degree of quenching intermediate between that of the lower lipid concentration (35 μM, with lower lipid to quencher molar ratio) and that of the same lipid composition but with the receptor. These findings indicate that the AChR promotes lateral segregation of DPPC from 7-SLPC, diminishing the degree of DPH quenching. The reduced quenching in all Chol-containing samples, and especially in those having AChR (even at high temperatures), indicates that the lipid domain-promoting effect of the AChR is potentiated by Chol and vice versa.

In addition to differences in the height of the quenching curves, a drastic increase in quenching was observed near the phase transition temperature of systems whose magnitude and position depended only slightly on liposome composition. A shift of the transition zone to higher temperatures was clearly observed in liposomes containing *both* Chol and AChR, suggesting a significant increase in the stability of DPPC domains when both Chol and AChR are present. As expected, most samples displayed similar quenching values beyond 40 °C, most likely owing to the melting and ideal mixing of components (i.e., quencher and fluorescence probe). The only exception was the sample containing both Chol and AChR, where DPPC domains did not melt fully up to 58 °C.

Anisotropy of DPH. Steady-state DPH anisotropy (or polarization) has been extensively used since early days (*38*) to determine the phase transition of phospholipids because of the drastic changes in fluorescence anisotropy occurring at, or close to, the transition temperature (T_m). In an ordered lipid environment DPH molecules have a restricted rotational reorientation yielding high values of fluorescence anisotropy which abruptly decrease when the lipid matrix melts. This totally independent method, which relies on different assumptions, yielded results in full agreement with those of the quenching assays with regard to the lipid domain-promoting ability of the AChR and Chol on DPPC/DOPC systems (Figure 2A). Liposomes with the lowest (or highest) values of DPH quenching displayed the lowest (or highest) values of anisotropy of DPH, respectively; intermediate anisotropy curves were in the same order as their quenching counterparts (compare Figures 1A and 2A). A Boltzman-type equation was adjusted to the experimental anisotropy data and inflection points, furnishing the T_m of the different mixtures (*26*) (Table 2). As expected, a shift of T_m to higher temperatures was observed with increasing DPPC/DOPC molar ratio. For samples with equivalent lipid composition, T_m was higher in samples having Chol or AChR and highest when both Chol and AChR were present, reinforcing the notion that their effect on lipid segregation, as observed in the DPH quenching experiments, is additive. These results agree with our hypothesis that when AChR and Chol are present, a larger fraction of DPH is surrounded by an ordered phase owing to the increase in the area occupied by the DPPC domains.

PyPC Excimer to Monomer Fluorescence Ratio (E/M). We also investigated lipid organization and fluidity in reconsti-

Table 2: Transition Temperatures (T_m) of the DPPC/DOPC System Calculated from DPH Fluorescence Anisotropy in the Presence and Absence of Chol and AChR[a]

molar ratio	AChR	final lipid concn (μM)	T_m (°C)
DPPC/DOPC			
41:59		27	22.1
60:40		40	29.6
60:40	+	40	31.2
DPPC/DOPC/Chol			
41:59:20		35	26.6
60:40:20		48	32.6
60:40:20	+	48	34.4

[a] The lipid to protein molar ratio was 500:1.

tuted membranes by using a pyrene-labeled PC, a lipid probe having the fluorophore attached at the end of the 10-carbon acyl chain. This fluorescent pyrene-labeled lipid partitions favorably into lipid−fluid phases (*39*−*41*) and tends to form probe-enriched domains ("patches") laterally segregated from lipids in the gel state (*41*, *42*). Furthermore, PyPC displays a phase behavior similar to that of an unsaturated lipid with a low solubility in gel state bilayers, which is usually attributed to the poor fit of the pyrene moiety into the tightly packed lipids in the gel state (*39*). A very useful trait of pyrene probes, PyPC included, is that they form excimers when a molecule in the excited state collides with a molecule in the ground state. This phenomenon depends on both concentration and lateral diffusion of the probe in the lipid matrix (*39*, *41*, *43*, *44*). Consequently, experimental measurement of *E*/*M* can be effectively used to sense changes in the physical state and fluidity of the bilayer. *E*/*M* may increase by a local (or "apparent") augmented concentration of the probe owing to lateral segregation from the gel state into probe-enriched domains (clusters) and/or by an enhanced diffusion rate (fluidity).

We measured the effect of AChR on the lateral organization of DPPC/DOPC bilayers by comparing the *E*/*M* of AChR-free and AChR-containing samples, respectively. Figure 3A shows the *E*/*M* vs temperature plot for DPPC, DOPC, and DPPC/DOPC mixtures, with and without AChR. When pure DPPC bilayers were initially cooled, the high apparent concentration of the probe owing to its clustering from the gel state yields higher *E*/*M* values than those in the liquid state neat DOPC. In the latter case, the probe is distributed homogeneously and has a low apparent concentration, which should match its actual concentration. Upon heating DPPC bilayers, the increased diffusion rate gave rise to an increase in *E*/*M* until the phase transition was reached, at which point *E*/*M* decreased abruptly owing to the disappearance of PyPC clusters. At this region, the decrease in the apparent concentration of the probe as a result of its partitioning and solubilization into the emerging liquid phase predominates over the increased diffusion rate by heating. Once the phase transition is complete, any further increment in temperature resulted in a steady increase in *E*/*M*. *E*/*M* increased smoothly in DOPC, since no phase transition occurs for this lipid in the entire temperature range. An intermediate behavior was observed for the assayed mixtures of DPPC/DOPC, although the decrease in *E*/*M* recorded for pure DPPC at the phase transition was abrupt; in samples containing only 20% DOPC it was remarkably smooth, and at 40% DOPC it almost disappeared. This strong influence of small amounts of DOPC on *E*/*M* is explained by the partition of the majority of PyPC molecules into the liquid DOPC phase. Once the liquid state was reached (i.e., beyond ≈40 °C), *E*/*M* values were similar for all mixtures since the probe is most likely homogeneously distributed.

Incorporation of AChR into DPPC/DOPC caused no substantial changes in *E*/*M* compared to similar AChR-free mixtures (Figure 3A). On the basis of this result it can be hypothesized that expansion of the DPPC domain upon addition of AChR (which should increase *E*/*M*) could be masked by the restricted diffusion rate caused by the protein (which should reduce *E*/*M*) in the now more rigid environment. To dissect between these two possibilities, *E*/*M* was also measured in pure DPPC AChR-containing bilayers, where the whole system is in the gel state at temperatures below ∼40 °C. No phase segregation or increment in the extent of the domain is possible under such conditions, and *E*/*M* can only be affected by changes in bilayer rigidity. *E*/*M* was found to be strongly reduced upon incorporation of AChR into these samples (Figure 3A) in this temperature regime, which can only be explained in terms of restricted diffusion caused by a more rigid DPPC matrix. From this evidence, the lack of changes in *E*/*M* values upon incorporation of AChR into DPPC/DOPC can be safely attributed to expansion of the DPPC domain. Since *E*/*M* is diffusion- and concentration-dependent, it reports both decreases in the diffusion rate of the probe owing to the rigidifying effect of AChR on DPPC domains and simultaneous increments in the apparent concentration of the probe owing to the expansion of the domains. Beyond the phase transition, *E*/*M* values were slightly lower in the AChR-containing liposomes, suggesting that the lipid matrix as well as the AChR-surrounding shell lipid is more rigid even in the liquid state.

Bilayer Organization in the POPA/POPC/AChR System

DPH Quenching. The temperature dependence of DPH quenching in POPA/POPC (Figure 1B) was quite different from that in DPPC/DOPC. Only a slight reduction in the degree of quenching was observed at low temperatures (i.e., <15 °C) whereas quenching remained relatively constant from 15 to 58 °C. Thus, changes in the lipid organization (i.e., melting and mixing of lipids) between 0 and 15 °C were smaller than in DPPC/DOPC system, and no distinguishable lipid reorganization occurred beyond this narrow temperature range. We attribute the different quenching behavior of the two lipid systems to the smaller difference in T_m between POPA and POPC than between DPPC and DOPC. In binary mixtures, the higher the difference between T_m, the higher the lateral segregation (*45*). To explore this in greater detail, we calculated the T_m of each lipid by measuring the anisotropy of DPH in pure DPPC, DOPC, POPA, and POPC liposomes (inset in Figure 1). We determined a T_m of 18.2 and 40.4 °C for POPA and DPPC, respectively, in accordance with literature values (*46*). However, the very low T_m values for POPC and DOPC (−4 and −19 °C, respectively; *46*) did not permit us to experimentally determine the corresponding values of these latter in an aqueous system. Accordingly, the difference in T_m between POPA and POPC is approximately 22 °C, whereas that between DPPC and DOPC is approximately 60 °C. Our current interpretation on the lack of additional quenching of DPH in the POPA/POPC system upon heating is that the

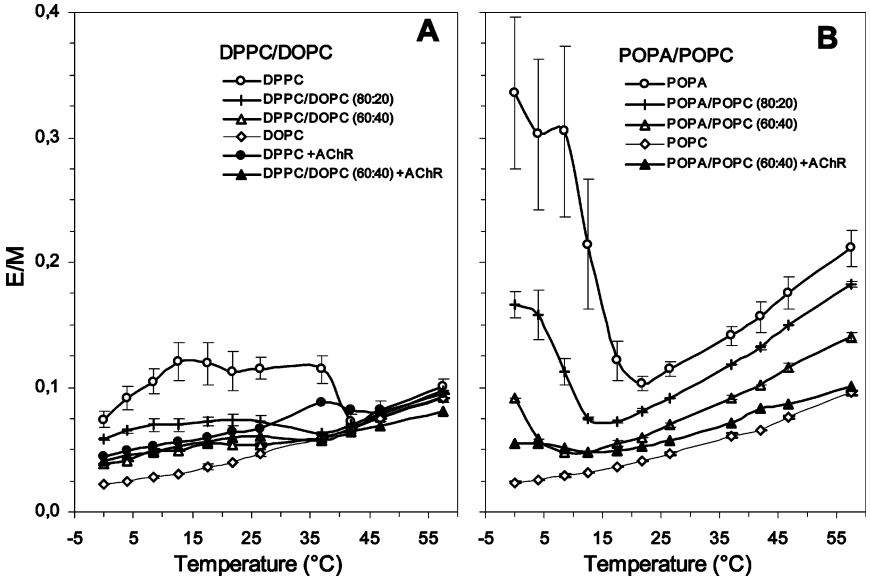

FIGURE 3: Temperature dependence of PyPC *E*/*M* in (A) DPPC/DOPC and (B) POPA/POPC, with or without AChR. *E*/*M* is expressed as F_{424nm}/F_{374nm}. The total lipid concentration and lipid to protein molar ratio in AChR-containing liposomes were 40 μM and 500:1, respectively. The PyPC concentration was 1 mol %. Error bars represent the SD of three independent experiments.

mixture is almost totally fluid beyond ~15 °C. The slight reduction in quenching recorded at the lowest temperatures assayed (<10−15 °C) in samples lacking Chol should thus correspond to the end of the phase transition zone. The portion of the quenching curves of POPA/POPC mixtures between 0 and 15 °C is therefore analogous to that found for DPPC/DOPC mixtures between 30 and 40 °C (compare panels A and B of Figure 1). The reduced quenching at low temperatures was only detected in the Chol-free samples because of the well-known ability of Chol to expand the phase transition (flattening the phase transition curves near T_m) and to rigidize the fluid state lipids (see DOPC/Chol 70:30 sample, inset in Figure 1).

Apart from the modest effect exerted by temperature on the quenching of DPH in all POPA/POPC mixtures, and unlike the findings for DPPC/DOPC liposomes, Chol did not have a statistically significant effect on DPH quenching in the POPA/POPC system, with or without AChR. However, there was a significant reduction in quenching in AChR-containing samples relative to similar samples lacking the receptor protein (Figure 1B). When AChR was added to a (73:27) POPA/POPC mixture, the resulting reconstituted liposomes (60:40) exhibited a significant reduction in DPH quenching, suggesting the promotion of quencher-depleted POPA microdomains. Liposomes with the same lipid composition but devoid of AChR displayed a higher degree of quenching, indicating that the observed effect is caused by the protein itself and not merely by the enhanced lipid to quencher ratio reached upon reconstitution.

Anisotropy of DPH. Addition of Chol caused an increase in DPH anisotropy above 10 °C, in both the absence and presence of AChR protein (Figure 2B). Incorporation of AChR into POPA/POPC membranes also caused an increase in DPH anisotropy. AChR-containing samples displayed lower absolute values of anisotropy than similar Chol-containing samples, indicating that the rigidizing effect induced by Chol is stronger than that exerted by the AChR protein. When AChR and Chol were present simultaneously, no additional increment in anisotropy was observed (Figure 2B). This is in agreement with the lack of changes in DPH quenching upon Chol incorporation. We interpret the difference between the DPPC- and the POPA-containing systems in terms of a competition between Chol and POPA for the same lipid shell sites around the AChR protein, as discussed below.

PyPC E/M. The effect of AChR protein on POPA/POPC was also investigated by measuring PyPC excimer formation. Although the temperature dependence of the *E*/*M* (Figure 3B) was qualitatively similar to that of the DPPC/DOPC system (Figure 3A), significant differences were observed in absolute terms. *E*/*M* was higher in neat POPA than in neat POPC throughout the whole temperature range, the difference being larger at temperatures of gel−liquid phase coexistence (i.e., <15−20 °C), as expected. This indicates that PyPC does not partition favorably in POPA, forming large "insoluble" patches at low temperatures that are maintained even at high temperatures, unlike the case of DPPC in the DPPC/DOPC system. The *E*/*M* in the POPA/POPC mixtures assayed was intermediate between those in POPA or POPC separately. Furthermore, the high *E*/*M* values observed in pure POPA at low temperatures were already observed to strongly diminish at 20−40% POPC. The high insolubility of PyPC in gel state POPA (which implies a large fraction of PyPC partitioned into liquid state POPC) explains why a small fraction of POPC has such a strong influence on *E*/*M*. The lack of overlap of *E*/*M* curves at temperatures >20 °C (i.e., when the lipid matrix is fully melted) suggests that even in the liquid phase PyPC must form clusters upon increasing the POPA:POPC ratio. The higher insolubility of PyPC in POPA relative to that in the assayed PCs is attributed to the influence of different polar headgroups on the interactions between the probe and phospholipids (*41*).

AChR incorporation attenuated the drop in *E*/*M* observed in POPA/POPC (60:40 molar ratio) at low temperatures (Figure 3B). This can be accounted for by a tighter packing of POPA molecules in the presence of AChR protein, which restricts probe diffusion. A drop in *E*/*M* could also be accounted for by a receptor-induced decrease in the size of

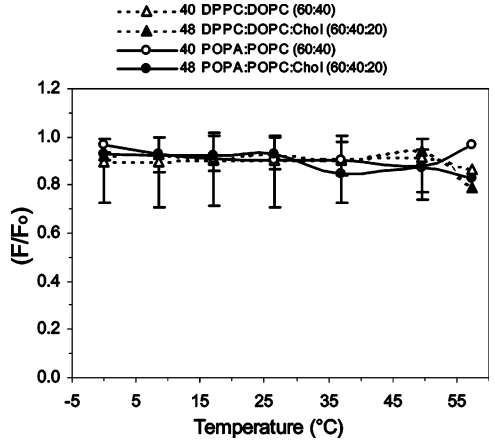

FIGURE 4: Quenching of the intrinsic fluorescence of AChR in DPPC/DOPC and POPA/POPC reconstituted liposomes, with or without Chol. Final lipid concentration (in μM) and molar ratio of components are indicated to the right of the symbols, respectively. The lipid to protein molar ratio was 500:1. Error bars represent the SD of three independent experiments.

the POPA domains, but this is unlikely to be the case in view of the results of DPH experiments, suggesting that the rigidizing effect of the AChR on vicinal PyPC is overriding. Taken together, DPH quenching and PyPC *E*/*M* experiments concur in pointing to the smaller size of POPA domains as compared to DPPC domains and to the rigidizing influence of the AChR on such domains.

Organization of the AChR Boundary Lipid

Quenching of AChR Intrinsic Fluorescence. Whereas quenching of DPH explores the overall organization of the bilayer, quenching of AChR fluorescence reports on the organization of the boundary (shell) lipid and the proximity of the quencher to the AChR protein. The degree of AChR quenching by 7-SLPC in either DPPC/DOPC or POPA/POPC mixtures did not vary in the 0−58 °C temperature range (Figure 4) even upon addition of Chol, suggesting the existence of a relatively stable shell of lipids shielding the AChR from quenching.

Förster Energy Transfer (FRET) from AChR to DPH. The good spectral overlap between the AChR intrinsic fluorescence emission (F_{330}) and DPH absorption (F_{424}) enabled us to employ FRET conditions (Figure 5) by exciting samples at the protein main absorption band (290 nm).

FRET, expressed as the ratio between extrinsic (DPH) fluorescence and intrinsic (AChR) emissions (F_{424}/F_{330}), increased slightly with increases in temperature and upon addition of Chol, especially in the POPA/POPC system. Higher temperatures can lead to higher FRET efficiency due to closer proximity of donor and acceptor fluorophores or to an increased quantum yield caused by redistribution of lipids. Since DPH partitions equally between liquid and solid lipid phases (*38*), the number of DPH molecules surrounding an AChR molecule can be expected to remain relatively constant; it is thus unlikely that a redistribution of fluorophores accounts for the observed increment in FRET upon heating the samples or upon addition of Chol. Assuming an even partition of DPH, variations in its quantum yield due to redistribution (and thus mixing) of lipids upon heating could account for the changes in FRET. We measured DPH fluorescence intensity in liposomes composed of pure DPPC, DOPC, POPA, or POPC. Figure 5 inset shows the relative quantum yield of DPH expressed as the ratio of fluorescence of the probe in DOPC and DPPC liposomes and in POPC and POPA liposomes, respectively. In either lipid system DPH fluorescence was higher in bilayers composed of the lipid with the lowest T_m (DOPC and POPC, respectively), particularly at lower temperatures.

To explain the higher FRET in the presence of Chol, we compared the quantum yield of DPH in Chol-containing and Chol-free mixtures composed of DPPC/DOPC and POPA/POPC, respectively. DPH fluorescence intensity was higher in the presence of Chol, especially for POPA/POPC membranes (Figure 5, inset). Chol also increased DPH fluorescence in the presence of quencher (7-SLPC) (Figure 5, inset), but the increment was more noticeable in DPPC/7-SLPC mixtures than in POPA/7-SLPC mixtures. An increase in DPH quantum yield cannot account entirely for the Chol-dependent increment in DPH fluorescence. Instead, we propose that Chol induces the segregation of DPPC in the DPPC/DOPC system but not of POPA in the POPA/POPC system. The increased DPH fluorescence in the DPPC/7-SLPC system can thus be most likely attributed to the presence of DPPC domains in which DPH is sheltered from the quencher. It is worth noting that an additional cause of increasing FRET (F_{424}/F_{330}) could be a lower quantum yield of AChR as temperature increases, relative to the quantum yield of DPH under the same conditions. Our experiments show that the quantum yield of both AChR and DPH diminished at the same rate with increasing temperature (data not shown). The fluorescence ratio (F_{424}/F_{330}) used to estimate FRET was then independent of changes in their quantum yield caused by heating. If this were not the case, F_{424}/F_{330} could be misjudging FRET.

The results of this series of experiments also suggest that the AChR is enclosed in lipid microdomains enriched in either DPPC or POPA; the two microdomains differ in size and segregate within a liquid phase enriched in either DOPC or POPC. As the temperature increases, the AChR-containing microdomains melt and those DPH molecules located in the DPPC- or POPA-enriched microdomain (having a relatively low quantum yield) become surrounded by an increasing proportion of DOPC or POPC molecules, respectively (in which milieu DPH displays a higher quantum yield). Thus, the enhanced quantum yield of a fraction of DPH molecules in the AChR microenvironment suffices to account for the slight increase in FRET with increasing temperature. These molecules are assumed to be within, or close to, the Förster distance, and they represent the fraction of fluorophores that can be excited by FRET upon exciting AChR Trp residues.

Energy Transfer from AChR to PyPC. We exploited the preference of PyPC for the liquid phase (*39*−*41*) to further investigate lipid organization within FRET distances from the AChR protein. Figure 6 shows the temperature dependence of FRET for both lipid systems, expressed as the ratio between the fluorescence of PyPC (M + E) and the fluorescence of AChR upon 290 nm excitation. FRET in pure DPPC/AChR remained approximately constant up to 25−30 °C (Figure 6A). Upon increasing the temperature the system began to melt and FRET decreased. This effect could be due to the temperature-dependent increase in the number of PyPC molecules removed from the vicinity of the AChR protein and their partition into the emerging pure DPPC-

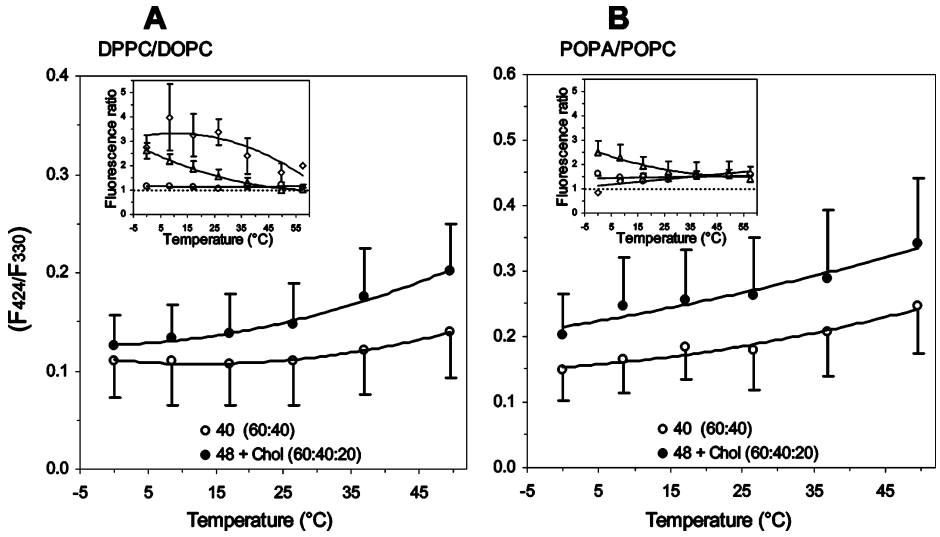

FIGURE 5: Temperature dependence of FRET from AChR to DPH, expressed as the ratio between the fluorescence intensity of DPH at 424 nm and the fluorescence intensity of AChR at 330 nm. Excitation wavelength = 290 nm. Total lipid concentration and molar ratio are indicated by the first figure on the left and that in parentheses, respectively. DPH concentration was 1 mol %. Error bars correspond to the SD of three independent experiments. Insets: Comparative quantum yield of DPH expressed as the fluorescence intensity ratio in different liposomes: (Δ) fluorescence in DOPC liposomes versus fluorescence in DPPC liposomes (A) and fluorescence in POPC versus fluorescence in POPA liposomes (B); (○) fluorescence in Chol-containing versus fluorescence in Chol-free liposomes of DPPC/DOPC (41:59 mol/mol) (A) and POPA/POPC (73:27 mol/mol) (B); (◇) fluorescence in Chol-containing versus fluorescence in Chol-free liposomes of DPPC/7-SLPC (41:59 mol/mol) (A) and POPA/POPC (73:27 mol/mol) (B). See Table 1 for detailed liposome composition. Error bars represent the SD of three independent experiments.

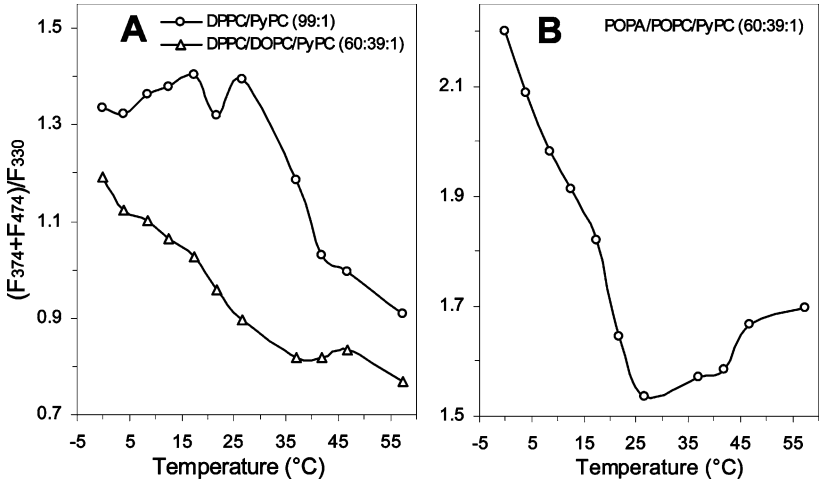

FIGURE 6: Energy transfer from AChR to PyPC as a function of temperature. FRET is expressed as the ratio between the fluorescence intensity of PyPC ($F_{374} + F_{474}$) and the fluorescence intensity of AChR (F_{330}). Excitation wavelength = 290 nm. Total lipid concentration and lipid to protein molar ratio of liposomes were 40 μM and 500:1, respectively. The PyPC concentration was 1 mol %.

enriched liquid phase, distant from donor AChR fluorophores (*47*). FRET was lower in the binary DPPC/DOPC/AChR mixture than in the single lipid (DPPC) system at any given temperature (Figure 6A), an observation that can be accounted for by the larger number of PyPC molecules partitioned into the DOPC-enriched liquid domain, separated from donor AChR molecules. As the temperature increased, FRET diminished, because of the partition of PyPC into the increasing liquid phase produced by the melting and mixing of DPPC with DOPC. As in pure "binary" DPPC/AChR liposomes, once the system is in the liquid state, further heating does not reduce FRET to the same extent, because the increased diffusion rate facilitates successful collisions between PyPC and AChR protein.

A similar temperature dependence of FRET was observed for POPA/POPC/AChR, although the drop at the phase transition temperatures was more abrupt (Figure 6B). This drastic diminution in FRET can be explained by the high insolubility of PyPC in POPA; an increasing number of PyPC molecules are excluded from the AChR surrounding POPA as they partition into the liquid phase POPC-enriched domain, which increases as a function of temperature (Figure 6B). As in DPPC/DOPC/AChR, the trend reverted once the system was totally melted, possibly due to the augmented diffusion rate in the liquid phase. In fact, FRET displayed a clear tendency to increase with increasing temperature when this system was in the liquid state.

DISCUSSION

In the present work we investigated the effect of AChR on lateral lipid segregation in reconstituted bilayers having lipids with different degrees of saturation and polar head-

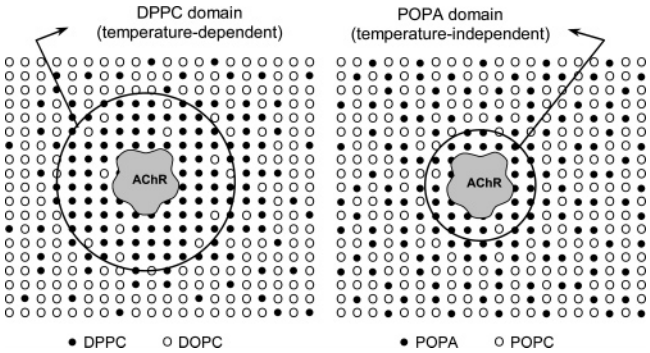

FIGURE 7: Scheme illustrating the proposed organization of lipids in bilayers of DPPC/DOPC (left) and POPA/POPC (right) containing the AChR protein.

groups. The AChR was found to increase the proportion of saturated enriched domains with a higher lateral packing density in bilayers composed of saturated and unsaturated lipid (DPPC/DOPC or POPA/POPC mixtures). The proportion of ordered lipid appears to be sensitive to the phase transition temperature and to the polar headgroup of the constitutive lipids (PC or PA). In the DPPC/DOPC system, in which the difference in transition temperature was larger than in the POPA/POPC system, the ordered phase-promoting effect of the AChR protein was more noticeable, suggesting that a larger fraction of the AChR-associated microdomain is in the gel or ordered phase. This leads us to postulate that in these binary lipid systems the AChR organizes its vicinal lipid shell, concentrating DPPC or POPA (in a gel, ordered state) in its immediate microenvironment. As a consequence, DOPC or POPC (in a liquid or disordered state) forms a separate phase (Figure 7). When temperature increases, the DPPC-ordered microdomains melt and mix with liquid DOPC-enriched microdomains. POPA-enriched domains, on the other hand, remain practically unperturbed in the temperature range studied. POPA-enriched microdomains are more stable at higher temperatures and are postulated to be smaller than DPPC-enriched domains.

The fact that DPPC−AChR microdomains are more temperature sensitive suggests that they are maintained predominantly by lipid−lipid interactions, the relative contribution of which diminishes upon heating and melting of the lipids. On the other hand, the thermal stability of the smaller POPA domains suggests that they are sustained primarily by more stable, lipid−protein interactions, and they reflect the influence of the phospholipid polar headgroup on the lipid−protein interaction.

The absence of additional quenching of DPH (Figure 1B) or AChR (Figure 4) upon heating the POPA/POPC system points to a fairly constant average distance between AChR and quencher within a wide temperature range. This observation is consistent with the hypothesis that a small number of POPA molecules interact with and surrounds each AChR molecule, as reported for the lipid shell of the AChR (40−50 molecules per receptor) (*48*, *49*). It is possible that such a reduced number of lipids remain around the protein because POPA−AChR interactions are stronger than POPA−POPC interactions; PA belongs to the category of high specificity groups of lipids interacting with the AChR (*48*). Hence, POPA molecules do not segregate by themselves from liquid-phase POPC (as seems to be the case with DPPC in the DPPC/DOPC system) in a binary, pure lipid system. It is thus the presence of the AChR that drives the phase separation and subsequent tight association of POPA with the protein moiety.

The relatively small headgroup of POPA should lead to the tight packing and restricted motion of the fatty acyl chains and, thus, to a more ordered, less fluid microenvironment. This can help to explain the positive effects of PA on AChR function in reconstituted systems, in which the resting, agonist-sensitive state of the AChR is predominantly formed. The resting state of the AChR is the form susceptible to agonist-induced conformational changes. No evident phase transition could be detected by the quenching assay, most likely because both the fraction of POPA molecules that surround the AChR and the fraction of molecules of DPH located in such lipid microdomain are too small.

In contrast to what was observed with the DPPC/DOPC system, the lack of any significant effect of Chol on DPH quenching and DPH anisotropy in the ternary POPA/POPC/AChR system indicates that AChR−vicinal POPA microdomains are maintained by POPA−protein interactions rather than by POPA−Chol interactions. This in turn suggests a possible competition between Chol and POPA for the same binding sites on the AChR protein, which could explain why no further decrease in DPH quenching or additional increase in anisotropy relative to the AChR- or Chol-containing samples is observed when *both* the protein and Chol are present. Chol can compete with phospholipids for AChR annular binding sites, and it can also bind to additional sites that are not accessible to phospholipids ("nonannular sites"; *50*−*52*). Studies from our laboratory (*52*, *53*) further characterized the physical state of the two classes of sites and the ability of fatty acids to displace phospholipids and cholesterol from distinct sites on the AChR surface.

The presence of distinct lipid classes in association with areas of AChR neurotransmitter receptor (macro)clusters was early reported in rat myotubes (*16*). A recent study (*54*) showed that Chol removal from ciliary neurons results in the dispersion of ordered lipid domains (interpreted within the context of the raft hypothesis) and α7-type neuronal AChR, suggesting that depletion of Chol reduces the forces responsible for the association of the receptor with ordered lipid domains. The AChR was also found to be resistant to cold detergent extraction (*54*) and to float with caveolin and flotillin (purported raft-marker proteins) in density gradients (*55*). In cellular systems, the delivery and clustering of the AChR at the plasma membrane have also been reported to be affected by the presence of Chol- and sphingolipid-enriched microdomains (*55*). In all of these cases, however, the dimensions of such domains were several microns wide, i.e., of the same order as the AChR (macro)clusters present in the fully developed peripheral synapse. The parallel set of cytochemical and biochemical studies did not, however, provide conclusive evidence that the purported AChR−lipid association occurred in situ.

Studies of AChR−lipid interactions in reconstituted systems provide information on a different scale. Fong and McNamee (*7*) correlated the ion flux function of reconstituted AChR with the order parameter of the bilayer, as measured by electron spin resonance techniques. Narayanaswami and McNamee (*51*) indicated that the AChR microenvironment exhibited a higher fluidity than the bulk lipid, and Sunshine and McNamee (*56*), also using reconstituted AChR, con-

cluded that the protein partitioned preferentially in fluid phase lipids. The lipid domains defined by these techniques comprise at most a few shells of lipid around each AChR protein. In contrast, subsequent fluorescence studies from our laboratory using the so-called general polarization (GP) of the probe Laurdan could address this issue in the native *Torpedo* AChR-rich membranes, showing that the AChR-vicinal lipids are more rigid and exhibit a lesser degree of water penetration than the bulk of the bilayer and that a single thermotropic phase with the characteristics of the liquid-ordered phase defines the AChR-rich postsynaptic membrane of fish electrocytes (*19*). daCosta et al. (*10*) reported that incorporation of AChR into model membranes leads to an increase in the percentage of non-hydrogen-bonded lipid ester carbonyl groups, in agreement with our results indicating that the AChR reduces water penetration at the interface level and enhances the density of the phospholipid headgroup packing and membrane order (*19*).

Early studies (*3*, *57*) reported that the anionic phospholipid PA is involved in the modulation of AChR function. The dianionic form of PA was found to be twice as effective as the monoanionic phospholipid in stimulating AChR-mediated ion flux in reconstituted systems (*28*, *58*), but the p*K* of PA does not appear to change in the presence of the AChR (*10*). PA stabilizes the AChR predominantly in the resting state (*5*, *11*, *29*, *57*). Membranes containing PA (and AChR) exhibit higher phase transition temperatures than those of nonfunctional bilayers composed of POPC alone, thus pointing to the tight packing of the lipid headgroups (*10*) and to the specificity and functional importance of PA. Poveda et al. (*11*) also found that the AChR affects phospholipid organization in reconstituted Chol-containing liposomes: In the absence of AChR they found an ideal mixing of lipids, whereas the presence of receptor protein directed lateral phase separation of certain phospholipids (e.g., DMPA) but not of others (DMPG, DMPC, DMPE), causing the formation of lipid domains segregated from the bulk lipid matrix. The ordering effect of the AChR is much greater in PA-containing membranes than in pure PC membranes (*10*). Our present results are in full agreement with the two latter studies.

The intrinsic fluorescence quenching experiments in the POPA/POPC system (Figure 4) upon substitution of POPC by 7-SLPC are in agreement with those reported by Chattopadhyay and McNamee (*59*) in DOPC/7-SLPC mixtures. But when DOPC was replaced by 7-SLPC in the DPPC/DOPC system, our quenching values were lower than those reported by these authors in pure DOPC. According to our current interpretation, the higher degree of AChR quenching in DOPC found by Chattopadhyay and McNamee (*59*) was due to the ideal mixing of quencher and lipid at room temperature, whereas the absence of segregated domains results in more efficient quenching of the AChR intrinsic fluorescence as shown in the present work. Taken together, these observations reinforce our hypothesis that DPPC−AChR microdomains in DPPC/DOPC are larger than POPA−AChR microdomains in POPA/POPC. This can be rationalized in a straightforward manner if one considers that, on average, the quencher is located more distant from the AChR in the former system.

The number of PA molecules in the shell region surrounding and interacting with the AChR has been reported to vary between 120 and 220 per AChR monomer (*11*). This is higher than the calculated number of lipids that an AChR molecule can accommodate in its immediate ("first-shell") perimeter if one takes into account the most recent structural data on the AChR transmembrane region (*49*; see also refs *1* and *2* for a discussion of this topic). The implication is that PA−AChR-enriched microdomains cannot be driven solely by hydrophobic lipid−protein interactions but possibly by additional interactions between the PA polar headgroup and extramembranous regions of the AChR (*3*), extending beyond the first-shell lipid ("annulus"). Despite the known high affinity of AChR for anionic lipids, the negative charge of PA alone has been deemed not to be responsible for specific interactions at the AChR−lipid interface (*60*, *61*), suggesting that this lipid might have complex and unique interactions with the protein. As discussed by Poveda et al. (*11*), electrostatic interactions do not suffice to account for the selectivity exhibited for binding of PA to the AChR: other classes of anionic phospholipids cannot substitute PA in domain segregation, despite having the same charge at neutral pH and identical fatty acid composition. Rather than electrostatic interactions alone, the selectivity must be determined by the interaction between the entire phospholipid headgroup and specific sites in the AChR protein.

Native *Torpedo* AChR-rich membranes are particularly enriched in Chol (see review in ref *20*), and Chol is known to stabilize the structure (*62*) and function (e.g., refs *5*, *30*, and *63*) of the AChR protein. Thus, the maintenance of an ordered phase in the AChR microenvironment (*19*, *52*) is likely to be modulated and promoted by the chemical activity of the neutral lipid, Chol (and other lipid domain-promoting sterols) in addition to anionic phospholipids such as PA, whereas alteration of AChR function by steroids (*21*, *22*, *24*, *25*) may be associated with the ability of the great majority of steroids to impair ordered lipid domain formation (*26*).

The effect of lipid lateral organization, and segregation in particular, on the structure and function of the AChR is still in need of clarification. Our results emphasize the notion that the AChR is key in determining the physical state of its immediate lipid microenvironment, the relevance of which is substantiated in the finding that relatively ordered lipids stabilize the AChR in a predominantly functional, resting conformation (*10*), whereas relatively fluid or disordered membranes favor the desensitized conformation (*5*, *10*). Our findings illustrate another facet of this issue, highlighting the ability of the AChR to determine, or at least strongly influence, the extension of the associated ordered lipid microdomains.

ACKNOWLEDGMENT

Thanks are due to Dr. Silvia Antollini for valuable discussions and comments.

REFERENCES

1. Barrantes, F. J. (2003) Modulation of nicotinic acetylcholine receptor function through the outer and middle rings of transmembrane domains, *Curr. Opin. Drug Discov. Devel. 6*, 620−632.
2. Barrantes, F. J. (2004) Structural basis for lipid modulation of nicotinic acetylcholine receptor function, *Brain Res. Rev. 47*, 71−95.

3. Fong T. M., and McNamee M. G. (1987) Stabilization of acetylcholine receptor secondary structure by cholesterol and negatively charged phospholipids in membranes, *Biochemistry 26*, 3871−3880.
4. Fernandez-Ballester, G., Castresana, J., Fernandez, A. M., Arrondo, J. L., Ferragut J. A., and Gonzales-Ros, J. M. (1994) A role for cholesterol as a structural effector of the nicotinic acetylcholine receptor, *Biochemistry 33*, 4065−4071.
5. Baenziger, J. E., Morris, M. L., Darsaut, T. E., and Ryan, S. E. (2000) Effect of membrane lipid composition on the conformational equilibria of the nicotinic acetylcholine receptor, *J. Biol. Chem. 275*, 777−784.
6. Addona, G. H., Sanderman, H., Kloczewiak, M. A., and Miller, K. W. (2003) Low chemical specifity of the nicotinic acetylcholine receptor sterol activation site, *Biochim. Biophys. Acta 1609*, 177−182.
7. Fong, T. M., and McNamee, M. G. (1986) Correlation between acetylcholine receptor function and structural properties, *Biochemistry 25*, 830−840.
8. Cantor, R. S. (1997) The lateral pressure profile in membranes: a physical mechanism of general anesthesia, *Biochemistry 36*, 2339−2344.
9. Dan, N., and Safran, S. A. (1998) Effect of lipid characteristics on structure of transmembrane protein, *Biophys. J. 75*, 1410−1414.
10. daCosta, C. J. B., Ogrel, A. A., McCardy, E. A., Blanton, M. P., and Baenziger, J. E. (2002) Lipid−protein interactions at the nicotinic acetylcholine receptor: a functional coupling between nicotinic receptors and phosphatidic acid containing lipid bilayer, *J. Biol. Chem. 277*, 201−208.
11. Poveda, J. A., Encinar, J. A., Fernández, A. M., Reyes Mateo, C., Ferragut, J. A. and Gonzáles-Ros, J. M. (2002) Segregation of phosphatidic acid-rich domains in reconstituted acetylcholine receptor membranes, *Biochemistry 41*, 12253−12262.
12. Simons, K., and Ikonen, E. (1997) Functional rafts in cell membranes, *Nature 387*, 569−572.
13. Brown, D. A., and London, E. (1998) Functions of lipid rafts in biological membranes, *Annu. Rev. Cell Dev. Biol. 14*, 111−136.
14. Chatterjee, S., Smith, E. R., Hanada, K., Stevens, V. L., and Mayor, S. (2001) GPI anchoring leads to sphingolipid-dependent retention of endocytosed proteins in the recycling endosomal compartment, *EMBO J. 20*, 1583−1592.
15. Sharma, P., Varma, R., Sarasij, R. C., Ira, Gousset, K., Krishnamoorthy, G., Rao, M., and Mayor, S. (2004) Nanoscale organization of multiple GPI-anchored proteins in living cell membranes, *Cell 116*, 577−589.
16. Scher, M. G., and Bloch, R. J. (1991) The lipid bilayer of acetylcholine receptor clusters of cultured rat myotubes is organized into morphologically distinct domains, *Exp. Cell Res. 195*, 79−91.
17. Marsh, D., and Barrantes, F. J. (1978) Immobilized lipid in acetylcholine receptor-rich membranes from *Torpedo marmorata*, *Proc. Natl. Acad. Sci. U.S.A. 75*, 4329−4333.
18. Marsh, D., Watts, A., and Barrantes, F. J. (1981) Phospholipid chain immobilization and steroid rotational immobilization in acetylcholine receptor-rich membranes from *Torpedo marmorata*, *Biochim. Biophys. Acta 645*, 97−101.
19. Antollini, S. S., Soto, M. A., Bonini de Romanelli, I., Gutiérrez-Merino, C., Sotomayor, P. and Barrantes, F. J. (1996) Physical state of bulk and protein-associated lipid in nicotinic acetylcholine receptor-rich membrane studied by Laurdan generalized polarization and fluorescence energy transfer, *Biophys. J. 70*, 1275−1284.
20. Barrantes, F. J. (1989) The lipid environment of the nicotinic acetylcholine receptor in native and reconstituted membranes, *Crit. Rev. Biochem. Mol. Biol. 24*, 437−478.
21. Bouzat, C., and Barrantes, F. J. (1993) Acute exposure of nicotinic acetylcholine receptors to the synthetic glucocorticoid dexamethasone alters single-channel gating properties, *Mol. Neuropharmacol. 3*, 109−116.
22. Bouzat, C., and Barrantes, F. J. (1993) Hydrocortisone and 11-desoxycortisone modify acetylcholine receptor channel gating, *NeuroReport 4*, 143−146.
23. Bouzat, C., and Barrantes, F. J. (1996) Modulation of muscle nicotinic acetylcholine receptor by the glucocorticoid hydrocortisone: Possible allosteric mechanism of channel blockade, *J. Biol. Chem. 271*, 25835−25841.
24. Garbus, I., Bouzat, C., and Barrantes, F. J. (2001) Steroids differentially inhibit the nicotinic acetylcholine receptor, *NeuroReport 12*, 227−231.
25. Garbus, I., Roccamo, A. M., and Barrantes, F. J. (2002) Identification of threonine422 in transmembrane domain αM4 of the nicotinic acetylcholine receptor as a possible site of interaction with hydrocortisone, *Neuropharmacology 43*, 65−73.
26. Wenz, J. J., and Barrantes, F. J. (2003) Steroid structural requirements for stabilizing or disrupting lipid domains, *Biochemistry 42*, 14267−14276.
27. Rietveld, A., and Simons, K. (1998) The differential miscibility of lipids as the basis for the formation of functional membrane rafts, *Biochim. Biophys. Acta 1376*, 467−479.
28. Sunshine, C., and McNamee, M. G. (1992) Lipid modulation of nicotinic acetylcholine receptor function: the role of neutral and negatively charged lipids, *Biochim. Biophys. Acta 1108*, 240−246.
29. Ryan, S. E., Demers, C. N., Chew, J. P., and Baenziger, J. E. (1996) Structural effects of neutral and anionic lipids on the nicotinic acetylcholine receptor. An infrared difference spectroscopy study, *J. Biol. Chem. 271*, 24590−24597.
30. Barrantes, F. J. (1982) Interactions between the acetylcholine receptor and the non-receptor, peripheral nu-peptide (Mr 43000), in *Neuroreceptors* (Hucho F., Ed.) pp 315−328, De Gruyter, Berlin and New York.
31. Ochoa, E. L. M., Dalziel, A. W., and McNamee, M. G. (1983) Reconstitution of acetylcholine receptor function in lipid vesicles of defined composition, *Biochim. Biophys. Acta 727*, 151−162.
32. Lowry, O. H., Rosebrough, N. J., Farr, A. L., and Randall, R. J. (1951) Protein measurement with the folin phenol reagent, *J. Biol. Chem. 193*, 265−275.
33. Bligh, E. G., and Dyer, W. J. (1959) A rapid method of total lipid extraction and purification, *Can. J. Biochem. Physiol. 37*, 910−917.
34. Rouser, G., Fleisher, S., and Yamamoto, A. (1970) Two-dimensional thin layer chromatographic separation of polar lipids and determination of phospholipids by phosphorous analysis of spots, *Lipids* 5, 494−496.
35. Laemmli, U. K. (1970) Cleavage of structural proteins during the assembly of the head of bacteriophage T4, *Nature 227*, 680−685.
36. Xu, X., and London, E. (2000) The effect of sterol structure on membrane lipid domain reveals how cholesterol can induce lipid domain formation, *Biochemistry 39*, 843−849.
37. Xu, X., Bittman, R., Duportail, G., Heissler, D., Vilchezes, C., and London, E. (2001) Effect of structure of sterol and sphingolipids on the formation of ordered sphingolipids/sterol domain (rafts), *J. Biol. Chem. 276*, 33540−33546.
38. Lentz, B. R., Barenholz, Y., and Thompson, T. E. (1976) Fluorescence depolarization studies of phase transitions and fluidity in phospholipid bilayers. 2. Two-component phosphatidylcholine liposomes, *Biochemistry 15*, 4529−4537.
39. Somerharju, P. J., Virtanen, J. A., Eklund, K. K., Vainio, P., and Kinnunen, P. K. J. (1985) 1-palmitoyl-2-pyrenedecanoyl glycerophospholipids as membrane probes: evidence for regular distribution in liquid-crystalline phosphatidylcholine bilayers, *Biochemistry 24*, 2773−2781.
40. Jones, M. E., and Lentz, B. R. (1986) Phospholipid lateral organization in synthetic membranes as monitored by pyrene-labeled phospholipids: Effects of temperature and prothrombin fragment 1 binding, *Biochemistry 25*, 567−574.
41. Koivusalo, M., Alvesalo, J., Virtanen, J. A., and Somerharju, P. (2004) Partitioning of pyrene-labeled phospho- and sphingolipids between ordered and disordered bilayer domains, *Biophys. J. 86*, 923−935.
42. Holopainen, J. M., Lehtonen, J. Y. A., and Kinnunen, P. K. J. (1997) Lipid microdomains in dimyristoylphosphatidylcholine-ceramide liposomes, *Chem. Phys. Lipids 88*, 1−13.
43. Galla, H. J., and Hartmann, W. (1980) Excimer-forming lipids in membrane research, *Chem. Phys. Lipids 27*, 199−219.
44. Somerharju, P. (2002) Pyrene-labeled lipids as tools in membrane biophysics and cell biology, *Chem. Phys. Lipids 116*, 57−74.
45. London, E., and Brown, D. A. (2000) Insolubility of lipids in Triton X-100: Physical origin and relationship to sphingolipid/cholesterol membrane domains (rafts), *Biochim. Biophys. Acta 1508*, 182−195.
46. Marsh, D. (1990) *Handbook of Lipid Bilayers*, CRC Press, Boston, FL.
47. Pedersen, S., Jorgensen, K., Baekmark, T. R., and Mouritsen, O. G. (1996) Indirect evidence for lipid-domain formation in the transition region of phospholipid bilayers by two-probe fluorescence energy transfer, *Biophys. J. 71*, 554−560.

48. Ellena, J. F., Blazing, M. A., and McNamee, M. G. (1983) Lipid−protein interactions in reconstituted membranes containing acetylcholine receptor, *Biochemistry 22*, 5523−5535.
49. Mantipragada, S. B. L., Horváth, I., Arias, H. R., Schwarzmann, G, Sandhoff, K., Barrantes, F. J., and Marsh D (2003) Lipid−protein interactions and the effect of local anaesthetics in acetylcholine receptor-rich membranes from *Torpedo marmorata* electric organ, *Biochemistry 42*, 9167−9175.
50. Jones, O. T., and McNamee, M. G. (1988) Annular and nonannular binding sites for cholesterol associated with the nicotinic acetylcholine receptor, *Biochemistry 27*, 2364−2374.
51. Narayanaswami, V., and McNamee, M. G. (1993) Protein−lipid interaction and *Torpedo californica* nicotinic acetylcholine receptor function: 2. Membrane fluidity and ligand-mediated alteration in the accessibility of gamma subunit cysteine residues to cholesterol, *Biochemistry 32*, 12420−12427.
52. Antollini, S. S., and Barrantes, F. J. (1998) Disclosure of discrete sites for phospholipids and sterols at the protein−lipid interface in native acetylcholine receptor rich-membrane, *Biochemistry 37*, 16653−16662.
53. Antollini, S. S., and Barrantes, F. J. (2002) Unique effects of different fatty acid species on the physical properties of the *Torpedo* acetylcholine receptor membrane, *J. Biol. Chem. 277*, 1249−1254.
54. Brusés, J. L., Chauvet, N., and Rutishauser, U. (2001) Membrane lipid rafts are necessary for the maintenance of the alfa-7 nicotinic acetylcholine receptor in somatic spines of ciliary neurons, *J. Neurosci. 21*, 504−512.
55. Marchand, S., Devillers-Thiery, A., Pons, S., Changeux, J.-P., and Cartaud, J. (2002) Rapsyn escorts the nicotinic acetylcholine receptor along the exocytic pathway via association with lipid rafts, *J. Neurosci. 22*, 8891−8901.
56. Sunshine, C., and McNamee, M. G. (1994) Lipid modulation of nicotinic acetylcholine receptor function: The role of membrane lipid composition and fluidity, *Biochim. Biophys. Acta 1191*, 59−64.
57. Criado, M., Eibl, H., and Barrantes, F. J. (1984) Functional properties of the acetylcholine receptor incorporated in model lipid membranes. Differential effects of chain length and head group of phospholipids on receptor affinity states and receptor-mediated ion translocation, *J. Biol. Chem. 259*, 9188−9198.
58. Bhushan, A., and McNamee, M. G. (1993) Correlation of phospholipid structure with functional effects on the nicotinic acetylcholine receptor. A modulatory role for phosphatidic acid, *Biophys. J. 64*, 716−723.
59. Chattopadhyay, A., and McNamee, M. G. (1991) Average membrane penetration depth of tryptophan residues of the nicotinic acetylcholine receptor by the parallax method, *Biochemistry 30*, 7159−7164.
60. Raines, D. E., and Miller, K. W. (1993) The role of charge in lipid selectivity for the nicotinic acetylcholine receptor, *Biophys J. 64*, 632−641.
61. daCosta, C. J. B., Wagg, I. D., McKay, M. E., Blanton, M. P., and Baenziger, J. E. (2004) Phosphatidic acid and phosphatidylserine have distinct structural and functional interactions with the nicotinic acetylcholine receptor, *J. Biol. Chem. 279*, 14967−14974.
62. Artigues, A., Villar, M. T., Fernández, A. M., Ferragut, J. A., and González-Ros, J. M. (1989) Cholesterol stabilizes the structure of the nicotinic acetylcholine receptor reconstituted in lipid vesicles, *Biochim. Biophys. Acta 985*, 325−330.
63. Dalziel, A. W., Rollins, E. S., and McNamee, M. G. (1980) The effect of cholesterol on agonist-induced flux in reconstituted acetylcholine receptor vesicles, *FEBS Lett. 122*, 193−198.

BI048026G